AMERICAN SOCIETY FOR MICROBIOLOGY | Journal of Virology®

VIRUS-CELL INTERACTIONS

Disassembly of the TRIM23-TBK1 Complex by the Us11 Protein of Herpes Simplex Virus 1 Impairs Autophagy

Xing Liu,[a] Rachel Matrenec,[a] Michaela U. Gack,[b] Bin He[a]

[a]Department of Microbiology and Immunology, University of Illinois College of Medicine, Chicago, Illinois, USA
[b]Department of Microbiology, The University of Chicago, Chicago, Illinois, USA

ABSTRACT The Us11 protein encoded by herpes simplex virus 1 (HSV-1) functions to impair autophagy; however, the molecular mechanisms of this inhibition remain to be fully established. Here, we report that the Us11 protein targets *tripartite motif* protein 23 (TRIM23), which is a key regulator of autophagy-mediated antiviral defense mediated by TANK-binding kinase 1 (TBK1). In virus-infected cells, the Us11 protein drastically reduces the formation of autophagosomes mediated by TRIM23 or TBK1. This autophagy-inhibitory effect is attributable to the binding of the Us11 protein to the ARF domain in TRIM23. Furthermore, such interaction spatially excludes TBK1 from the TRIM23 complex that also contains heat shock protein 90 (Hsp90). When stably expressed alone in host cells, the Us11 protein recapitulates the observed phenotypes seen in cells infected with the US11-expressing or wild-type virus. Consistent with this, expression of the Us11 protein promotes HSV-1 growth, while expression of TRIM23 restricts HSV-1 replication in the absence of US11. Together, these results suggest that disruption of the TRIM23-TBK1 complex by the Us11 protein inhibits autophagy-mediated restriction of HSV-1 infection.

IMPORTANCE Autophagy is an evolutionarily conserved process that restricts certain intracellular pathogens, including HSV-1. Although HSV-1 is well known to inhibit autophagy, little is known about the precise molecular mechanisms of autophagy inhibition. We demonstrate that the Us11 protein of HSV-1 spatially disrupts the TRIM23-TBK1 complex, which subsequently suppresses autophagy and autophagy-mediated virus restriction. Thus, expression of the Us11 protein facilitates HSV-1 replication. These data unveil new insight into viral escape from autophagy-mediated host restriction mechanisms.

KEYWORDS herpes simplex virus, autophagy, viral replication, virus-host interactions

Autophagy is a conserved process that eliminates misfolded proteins, damaged organelles, or intracellular pathogens, including certain viruses (1, 2). Once initiated, the host cell engulfs cytosolic contents in double-membrane vesicles destined for clearance. This process depends on the interaction of Beclin1 with the class III phosphatidylinositol 3-kinase VPS34, which, along with autophagy-related protein 14 (ATG14) and vacuolar protein sorting 15 (VPS15), drives autophagosome formation. Consequently, autophagosomes undergo fusion for lysosomal degradation (2).

Available evidence suggests that a complex program is in operation where a network of proteins mediates autophagy (1–3). For example, double-stranded RNA-dependent protein kinase R (PKR) is activated in response to herpes simplex virus 1 (HSV-1) (4, 5). As a result, phosphorylation of the α subunit of translation initiation 2 (eIF2α) by PKR arrests protein synthesis and induces autophagy (4, 6). Accordingly, genetic deletion or inactivation of PKR abrogates autophagy (6, 7). In addition, TANK-binding kinase 1 (TBK1), which is essential for type I interferon (IFN) induction (8, 9), is important for autophagy. Notably, TBK1 facilitates the recruitment of a selected cargo

Citation Liu X, Matrenec R, Gack MU, He B. 2019. Disassembly of the TRIM23-TBK1 complex by the US11 protein of herpes simplex virus 1 Impairs autophagy. J Virol 93:e00497-19. https://doi.org/10.1128/JVI.00497-19.

Editor Richard M. Longnecker, Northwestern University

Address correspondence to Bin He, tshuo@uic.edu.

Received 23 March 2019
Accepted 3 June 2019
Accepted manuscript posted online 12 June 2019
Published 13 August 2019

to autophagy receptors, such as p62, nuclear dot protein 52 kDa (NDP52), or optineurin via direct interaction and phosphorylation of these receptor proteins (10–12). Recent work revealed that TBK1 is subjected to activation by cellular TRIM23 that regulates autophagy induction in response to multiple RNA viruses and DNA viruses, including HSV-1 (10).

HSV-1 is a large DNA virus that usually replicates in the epithelium of mucosal tissues and establishes latency in neurons of the peripheral nervous system (11). Primary infection or reactivation initiates a productive cycle, with sequential expression of HSV-1 genes that work cooperatively (12). Among them is the $\gamma_1$34.5 gene product that precludes translation arrest mediated by PKR (4, 5). In doing so, HSV-1 $\gamma_1$34.5 redirects protein phosphatase 1 (PP1) to dephosphorylate eIF2α (13, 14), which has been linked to the inhibition of autophagy (6). Moreover, the $\gamma_1$34.5 protein binds to Beclin1 to block autophagy, which mediates HSV-1 virulence *in vivo* (15). This is reported to dampen antigen presentation or CD4$^+$ T cell activation (16, 17). Of note, it has been reported that the Us11 protein of HSV-1 also perturbs autophagy by inhibition of PKR (18).

Previous work demonstrated that HSV-1 US11 is a late (γ_2) protein whose expression depends on viral DNA replication (19). One of the many functions of US11 (20–24) is to prevent the cessation of protein synthesis. This requires its interaction with PKR or cellular protein activator of protein kinase R (PACT), which results in the inhibition of eIF2α phosphorylation (25, 26). When expressed as an early (α) protein, the Us11 protein rescues viral growth in the absence of $\gamma_1$34.5 (27–29). In a screen for novel US11 functions, we recently identified that the Us11 protein negatively modulates TBK1 activity, which reduces IFN-α/β expression in virus-infected cells (30). TBK1 pathway inhibition by US11 contributes to viral replication (30). However, the underlying events of TBK1 inhibition by US11 remain incompletely understood. In this study, we report that US11 inhibits autophagy-mediated antiviral restriction by functional interruption of the TBK1 axis. In particular, US11 interacts with TRIM23 and blocks TBK1 assembly into a functional TRIM23 complex required for autophagy induction. These results reveal a new mechanism through which HSV-1 neutralizes host restriction in infected cells.

RESULTS

HSV-1 US11 interferes with TBK1-mediated autophagy induction in virus-infected cells. While it has been well established that TBK1 is essential for the type I IFN response (8, 9), it also has been recently implicated in autophagy (10–12). To better understand the US11-TBK1 connection, we examined autophagy in TBK1$^{+/+}$ and TBK1$^{-/-}$ mouse embryonic fibroblast (MEF) cells in response to HSV-1 infection. As US11 functions coordinately with $\gamma_1$34.5 (31, 32), we sought to define its role in the absence of $\gamma_1$34.5. Specifically, we analyzed wild-type (WT) HSV-1, the $\gamma_1$34.5 null mutant ($\Delta\gamma_1$34.5), and the $\gamma_1$34.5 null mutant in which US11 is driven by the α47 promoter (EUs11). First, we evaluated autophagosome formation in cells transiently transfected with green fluorescent protein–microtubule-associated protein 1 light chain 3B (GFP-LC3B), which is processed and recruited to the autophagosome membrane during autophagy. As shown in Fig. 1A and B, rapamycin stimulation strongly increased the number of GFP-LC3B puncta in TBK1$^{+/+}$ cells but not in TBK1$^{-/-}$ cells, indicative of autophagy induction by TBK1. This pattern was mirrored by infection with $\Delta\gamma_1$34.5 but not wild-type HSV-1 or EUs11. We next measured conversion of endogenous LC3B-I to LC3B-II, the latter being the active, membrane-bound form required for autophagosome formation. Similar to rapamycin treatment, infection with $\Delta\gamma_1$34.5 increased the level of LC3B-II in TBK1$^{+/+}$ cells compared to that in mock-treated cells. Conversely, the LC3B-II levels in TBK1$^{+/+}$ cells infected with wild-type HSV-1, or EUs11, were similar to those in mock-infected cells (Fig. 1C and D). These changes were minimally detectable in TBK1$^{-/-}$ cells. Collectively, these results indicate that autophagy induction by HSV-1 is dependent on TBK1. Furthermore, these data suggest that US11 suppresses TBK1-dependent autophagy in HSV-1-infected cells.

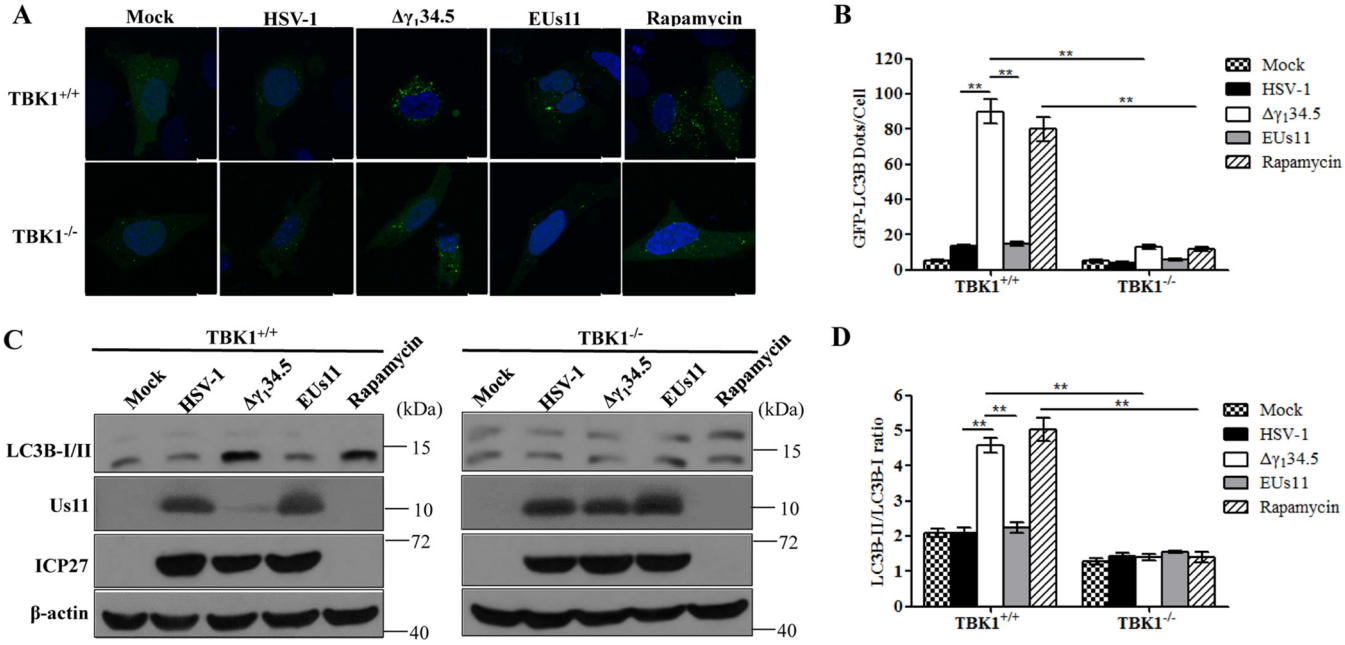

FIG 1 Us11 protein inhibits autophagy mediated by TBK1. (A) GFP-LC3B puncta formation in TBK1$^{+/+}$ and TBK1$^{-/-}$ MEFs. Cells transiently transfected with GFP-LC3B were infected with wild-type HSV-1, $\Delta\gamma_1$34.5, or EUs11 (MOI of 5) for 12 h or incubated with rapamycin (200 nM) for 10 h. Images were then captured. Nuclei were stained with DAPI (blue). Scale bar, 10 μm. (B) Quantitation of GFP-LC3B puncta formation. Results represent the mean number ± standard deviation (SD) of GFP-LC3B puncta per cell ($n = 20$). **, $P < 0.01$ (Student's t test). (C) Conversion of endogenous LC3B-I to LC3B-II. TBK1$^{+/+}$ or TBK1$^{-/-}$ MEFs were mock infected, infected with the indicated viruses, or stimulated with rapamycin as described for panel A. Cell lysates were then processed for Western blot analysis with antibodies against LC3B, US11, ICP27, and β-actin. (D) Densitometric quantification of LC3B-II/LC3B-I. The protein bands shown in panel C were quantified using NIH ImageJ software. The data are presented as the relative amount of LC3B-II and LC3B-I normalized to the total level of β-actin in each sample. The data are averages from three independent experiments and were statistically assessed by a two-tailed Student's t test. **, $P < 0.01$.

HSV-1 US11 prevents autophagy mediated by TRIM23 in virus-infected cells. TRIM23 was recently shown to activate autophagy by interacting with TBK1 (10). To determine whether US11 affects autophagy elicited by TRIM23, we measured GFP-LC3B puncta formation in HSV-1-infected cells. For this purpose, we utilized TRIM23$^{+/+}$ and TRIM23$^{-/-}$ MEF cells ectopically expressing GFP-LC3B. Figure 2A and B show that rapamycin effectively triggered formation of GFP-LC3B puncta in TRIM23$^{+/+}$ MEF cells, unlike mock treatment. Infection with $\Delta\gamma_1$34.5 also substantially induced GFP-LC3B puncta, which were detectable throughout the cytoplasm. In contrast, wild-type HSV-1, or EUs11, minimally enhanced GFP-LC3B puncta formation in TRIM23$^{+/+}$ cells compared to that of mock treatment of these cells. These activities were not evident in TRIM23$^{-/-}$ MEF cells, which are consistent with a pivotal role of TRIM23 in autophagy induction (10).

To confirm the results described above, we next examined LC3B-I to LC3B-II conversion in TRIM23$^{+/+}$ and TRIM23$^{-/-}$ MEF cells (Fig. 2C and D). As expected, rapamycin stimulation increased the protein abundance of endogenous LC3B-II in TRIM23$^{+/+}$ cells compared to that after mock treatment. While $\Delta\gamma_1$34.5 infection led to an increase in endogenous LC3B-II abundance, wild-type HSV-1 did not. Similarly, EUs11 did not increase the protein levels of LC3B-II in TRIM23$^{+/+}$ cells. These phenotypes correlated well with expression of US11, where viral infection was comparable, as measured by ICP27 expression. In TRIM23$^{-/-}$ MEF cells, the relative protein levels of LC3B-II remained unchanged under these experimental conditions. Consistent with the results obtained from TRIM23$^{+/+}$ and TRIM23$^{-/-}$ MEF, analysis of endogenous LC3B-I→LC3B-II conversion in infected human lung fibroblasts (HEL) in which TRIM23 was depleted using short hairpin RNA (shTRIM23) yielded similar results (Fig. 3A to C). We conclude from these experiments that the Us11 protein is crucial to inhibit autophagy mediated by TRIM23, particularly in the absence of $\gamma_1$34.5 in virus-infected cells.

The Us11 protein suppresses autophagy through exclusion of TBK1 from the TRIM23 complex. As a complex DNA virus, HSV-1 expresses a range of viral proteins in

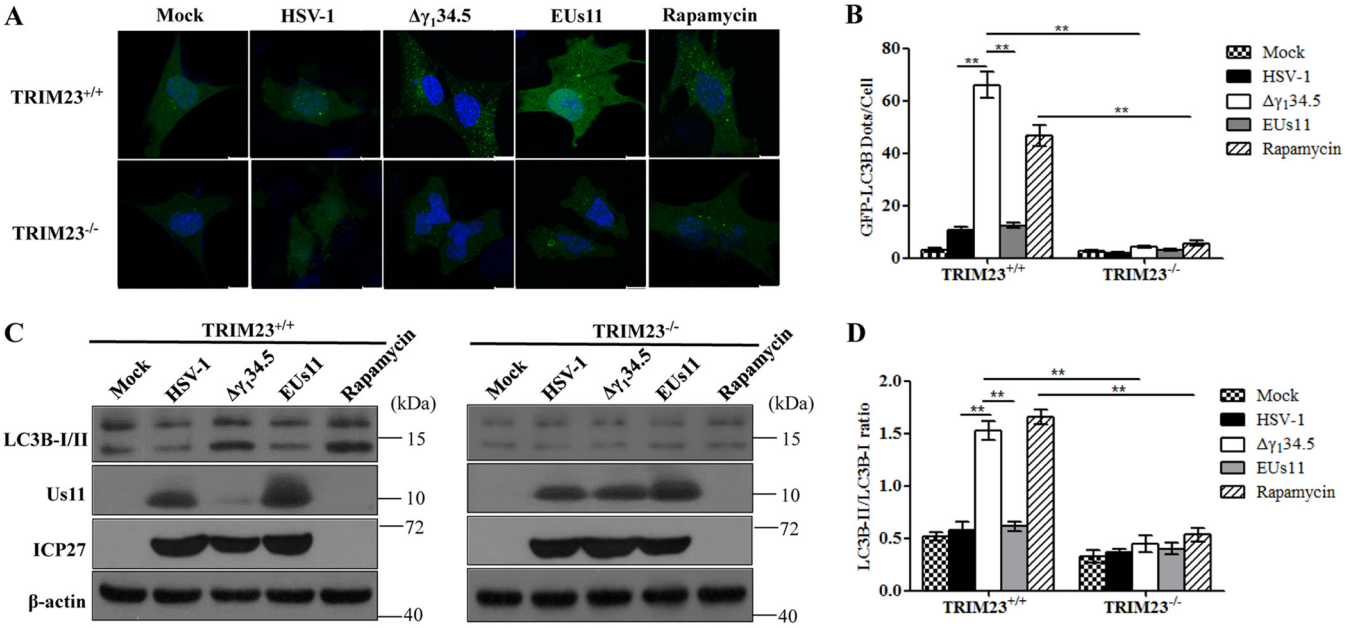

FIG 2 Us11 protein inhibits autophagy mediated by TRIM23. (A) GFP-LC3B puncta formation in TRIM23$^{+/+}$ and TRIM23$^{-/-}$ MEFs. Cells transiently transfected with GFP-LC3B were mock infected, infected with wild-type HSV-1, $\Delta\gamma_1$34.5, or EUs11 (MOI of 5) for 12 h, or incubated with rapamycin (200 nM) for 10 h. Images were then captured. Nuclei were stained with DAPI (blue). Scale bar, 10 μm. (B) Quantitation of GFP-LC3B puncta formation. Results represent the mean number $\pm$ SD of GFP-LC3B puncta per cell ($n = 20$). **, $P < 0.01$ (Student's t test). (C) Conversion of LC3B-I to LC3B-II. TRIM23$^{+/+}$ and TRIM23$^{-/-}$ MEFs were mock infected, infected with the indicated viruses, or stimulated with rapamycin as described for panel A. Cell lysates were then processed for Western blot analysis with antibodies against LC3B, US11, ICP27, and β-actin. (D) Quantification of LC3B-II/LC3B-I. The protein bands shown in panel C were quantified using NIH ImageJ software. The data are presented as the amount of LC3B-II relative to that of LC3B-I, normalized to the total amount of β-actin in each sample. The data are averages from three independent experiments and were statistically assessed by a two-tailed Student's t test. **, $P < 0.01$.

infected cells (12, 33). To delineate whether US11 works in the absence of any other viral proteins, we established stable MEF cell lines that express Flag-mCherry or Flag-US11-mCherry. After transient transfection with GFP-LC3B, we analyzed for autophagy induction triggered by rapamycin. As shown in Fig. 4A and B, cells, when left untreated, displayed only a few GFP-LC3B puncta. Treatment with rapamycin resulted in different patterns. In Flag-mCherry-expressing control cells, rapamycin treatment resulted in a large number of GFP-LC3B puncta; however, this increase was not visible in rapamycin-treated cells that expressed Flag-US11-mCherry. Consistent with these data, Flag-US11-mCherry expression reduced the conversion of endogenous LC3B-I to LC3B-II following rapamycin treatment (Fig. 4C). These activities were in parallel with the expression pattern of US11, where both full-length Flag-US11-mCherry and presumably proteolytic fragments were detected by Western blot analysis. Thus, the Us11 protein is able to block the formation of autophagosomes when expressed alone in host cells.

Previous work suggests that heat shock protein 90 (Hsp90) recruits and stabilizes TBK1 (34). Since TRIM23 binds to and activates TBK1 (10), we inferred that TRIM23 forms a functional complex with Hsp90 and TBK1, and that the integrity of this complex is disrupted by US11 to impair autophagy. As shown in Fig. 4D, anti-Hsp90 immunoprecipitation (IP) revealed that both TRIM23 and TBK1 coprecipitated with endogenous Hsp90 in control cells, suggesting the existence of an Hsp90-TRIM23-TBK1 complex. However, stable expression of US11 resulted in specific disappearance of TBK1 from the TRIM23 complex, where Hsp90 still remained bound to TRIM23. Therefore, HSV-1 US11 inhibits autophagy by disrupting the TRIM23-TBK1-Hsp90 complex.

The Us11 protein blocks recruitment of TBK1 by targeting the ARF domain in TRIM23. To probe the mechanism of US11 action, we assessed protein-protein interactions in cells transiently transfected with TRIM23, TBK1, Hsp90, US11, and controls. Figure 5A shows that TRIM23 interacted with Hsp90 when coexpressed in 293T cells. Similarly, TRIM23 associated with TBK1. These interactions were specific because

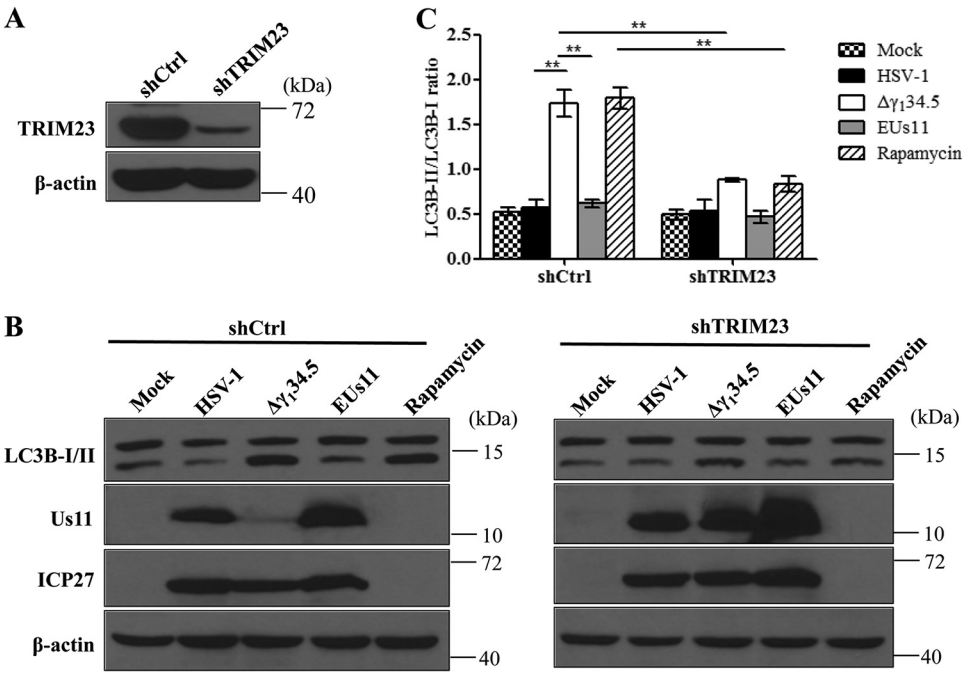

FIG 3 (A) TRIM23 depletion in human lung fibroblasts (HEL). Lysates of cells that were transduced with control shRNA (shCtrl) or shRNA targeting TRIM23 (shTRIM23) were subjected to Western blot analysis with antibodies against TRIM23 and β-actin. (B) Conversion of LC3B-I to LC3B-II. HEL cells, expressing shCtrl or shTRIM23, were mock infected, infected with wild-type HSV-1, $\Delta\gamma_1$34.5, or EUs11 (MOI of 5) for 12 h, or incubated with rapamycin (200 nM) for 10 h. Cell lysates were processed for Western blot analysis with antibodies against LC3B, US11, ICP27, and β-actin. (C) Quantification of LC3B-II/LC3B-I. The protein bands shown in panel B were quantified using NIH ImageJ software and are presented as the amount of LC3B-II relative to that of LC3B-I, normalized to the total amount of β-actin in each sample. The data are averages from three independent experiments and were statistically assessed by a two-tailed Student's *t* test. **, $P < 0.01$.

TRIM23 bound to neither enhanced GFP (EGFP) nor mCherry. When ectopically expressed together, TRIM23 interacted with Hsp90 and TBK1. Addition of US11 effectively displaced TBK1 in the TRIM23 complex with no visible effect on Hsp90 (Fig. 5B), which mirrored the effect of US11 on endogenous protein interactions (Fig. 4D). These results suggest that, by targeting TRIM23, HSV-1 US11 precludes incorporation of TBK1 into the TRIM23 complex.

To further address this question, we focused on characterizing the interaction of US11 and TRIM23. 293T cells were transfected with Flag-US11-mCherry along with V5-tagged TRIM23, followed by anti-V5 immunoprecipitation. As shown in Fig. 6A, US11 but not the control protein (Flag-mCherry) coprecipitated with TRIM23. To map the US11-binding region in TRIM23, we generated the following TRIM23 variants in which individual domains of the protein were deleted: TRIM23 lacking the N-terminal RING finger (ΔRING; amino acids [aa] 88 to 574), C-terminal ARF domain (ΔARF; aa 1 to 402), or both (CENTRAL; aa 88 to 402). Western blot analysis confirmed efficient expression of these mutant variants (Fig. 6B). When ectopically expressed, US11 precipitated with wild-type TRIM23 and its ΔRING mutant in immunoprecipitation assays (Fig. 6C). However, US11 failed to precipitate with the ΔARF or CENTRAL mutant, suggesting that the Us11 protein interacts with the ARF domain of TRIM23, which is necessary to bind TBK1 (10). In support of this, US11 efficiently bound to a TRIM23 mutant expressing only the ARF domain (ARF; aa 403 to 574) (Fig. 6C). Together, these results indicate that the Us11 protein binds to the C-terminal ARF domain of TRIM23 and thereby prevents TBK1 binding to TRIM23, which inhibits autophagy.

HSV-1 US11 downregulates TRIM23 and TBK1 protein abundance in virus-infected cells. Given the observed impact of US11, we further analyzed the TRIM23-TBK1-Hsp90 ternary complex in infected cells. Cells were mock infected or infected with

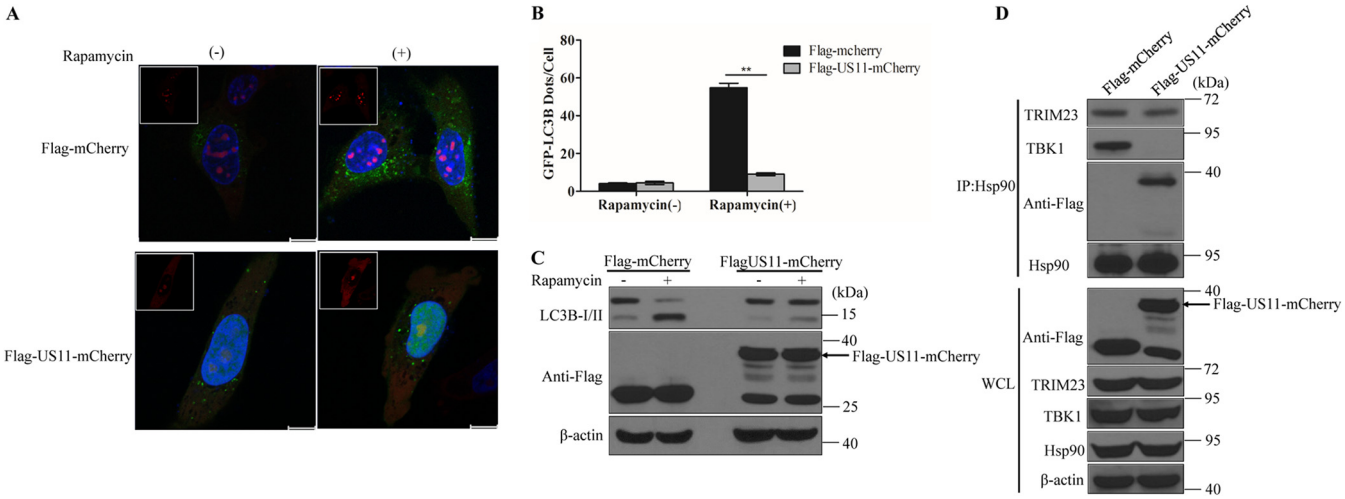

FIG 4 US11 inhibits autophagy in the absence of other HSV-1 proteins. (A) MEF cells stably expressing Flag-mCherry or Flag-US11-mCherry were transfected with GFP-LC3B. Cells were then incubated with rapamycin (200 nM) for 10 h and subjected to analysis by confocal microscopy (scale bar, 10 μm). Nuclei were stained with DAPI (blue). (B) Quantitation of GFP-LC3B puncta formation. Results represent the mean number ± SD of GFP-LC3B puncta per cell ($n = 20$). **, $P < 0.01$ (Student's t test). (C) Effects of US11 on endogenous LC3B-I to LC3B-II conversion induced by rapamycin. MEFs stably expressing Flag-mCherry or Flag-US11-mCherry were treated with DMSO or rapamycin for 10 h. Cell lysates were prepared and processed for Western blot analysis with antibodies against LC3B, Flag, and β-actin. (D) Effects of US11 on the TRIM23-TBK1-Hsp90 complex. MEFs stably expressing Flag-mCherry or Flag-US11-mCherry were processed for immunoprecipitation with Hsp90 antibody. Coprecipitated proteins and whole-cell lysates (WCL) were probed with antibodies against Hsp90, TRIM23, TBK1, Flag, and β-actin.

wild-type HSV-1, $\Delta\gamma_1$34.5, or EUs11. At 12 h postinfection, lysates of cells were subjected to immunoprecipitation and Western blot analysis. As illustrated in Fig. 7, Hsp90 associated with TRIM23 and TBK1 in mock-infected cells. Similarly, this interaction was seen in cells infected with $\Delta\gamma_1$34.5, where no US11 expression was detectable. However, in cells infected with wild-type HSV-1 or EUs11, TBK1 was not detectable in the Hsp90 complex, which coincided with the presence of US11 in the Hsp90 complex. TRIM23 remained associated with Hsp90 but at a reduced level. These results suggest that US11 was able to disrupt the assembly of TRIM23-TBK1-Hsp90 complex in virus-infected cells. Interestingly, the protein abundance of TRIM23 and TBK1 was lower in cells infected with wild-type HSV-1 or EUs11 than in cells mock infected or infected with $\Delta\gamma_1$34.5, suggesting that HSV-1 has evolved an additional mechanism to inhibit TRIM23 and TBK1 functions that is dependent on downregulating their protein abundances.

HSV-1 US11 rescues a viral growth defect imposed by TRIM23. Finally, we determined whether the US11-TRIM23 interaction affects HSV-1 replication. As illustrated in Fig. 8A, wild-type HSV-1 replicated efficiently in both TRIM23$^{+/+}$ and TRIM23$^{-/-}$ cells, reaching titers of 1×10^5 and 1×10^6 PFU/ml, respectively. However, $\Delta\gamma_1$34.5 replicated poorly (5×10^1 PFU/ml) in TRIM23$^{+/+}$ cells, although its growth was restored to a titer of 5×10^4 PFU/ml in TRIM23$^{-/-}$ cells. Notably, EUs11 displayed a different growth property. In TRIM23$^{+/+}$ cells, EUs11 reached a titer of 1×10^4 PFU/ml, demonstrating significantly increased growth compared to that of $\Delta\gamma_1$34.5. In TRIM23$^{-/-}$ cells, EUs11 replicated similarly to wild-type virus, reaching a titer of 4×10^5 PFU/ml. Consistent with this, these phenotypes were correlated with cytopathic effects (Fig. 8B). It appears that TRIM23 severely limits HSV-1 replication in the absence of $\gamma_1$34.5. However, US11 expression is able to largely override this blockade by TRIM23. These experimental results suggest that the Us11 protein functionally antagonizes cellular TRIM23 in HSV-1 infection.

DISCUSSION

In this work, we show that the US11-TRIM23 interaction is a regulatory step that controls HSV infection. Remarkably, such engagement with TRIM23 strongly suppresses autophagy. In support of this argument, we noted that, in contrast to wild-type HSV-1, the $\gamma_1$34.5 null mutant, which is unable to produce the Us11 protein, stimulated

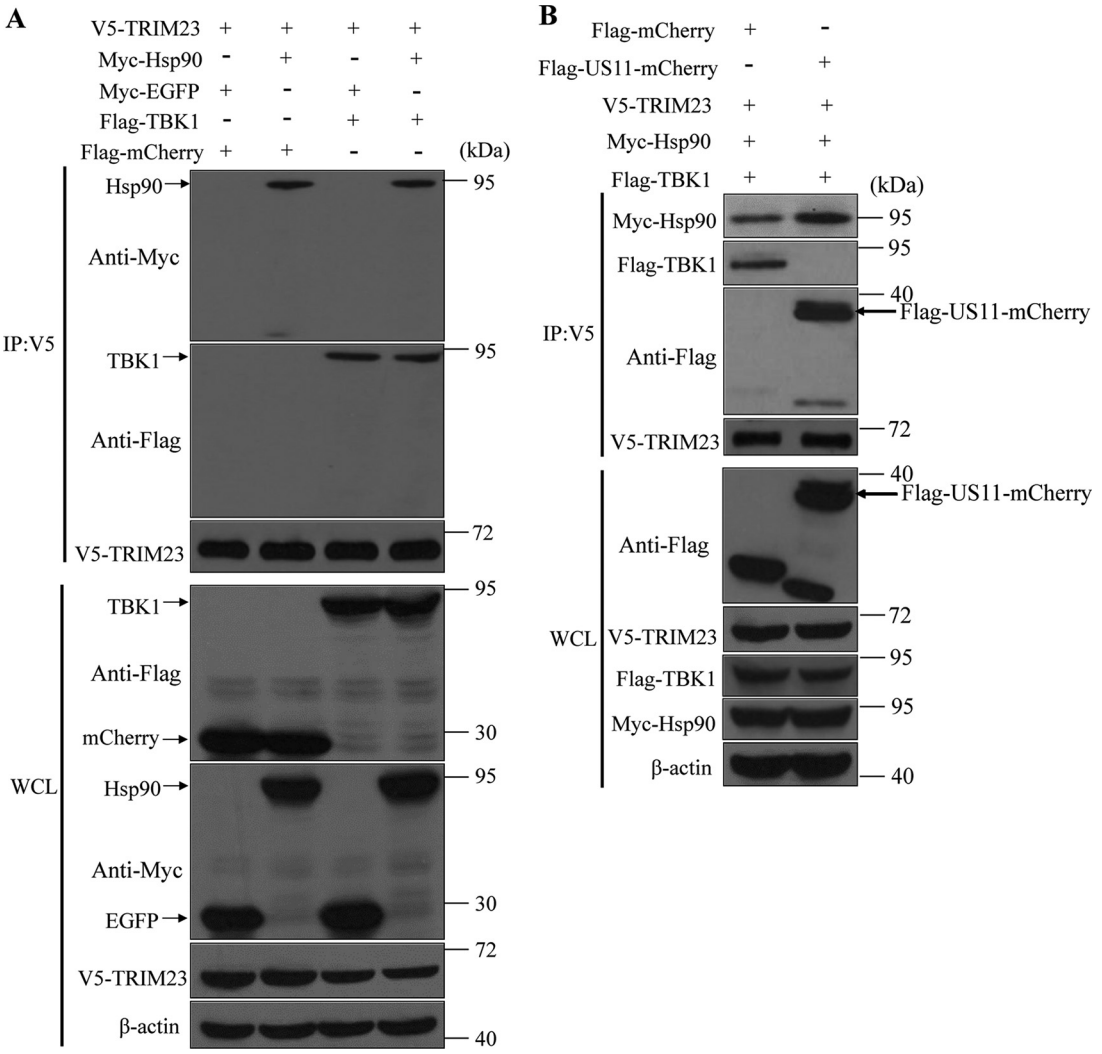

FIG 5 (A) TRIM23 associates with TBK1 and Hsp90. 293T cells were transfected with V5-TRIM23 along with Myc-Hsp90, Myc-EGFP, Flag-TBK1, and Flag-mCherry. At 36 h after transfection, cells were processed for immunoprecipitation with anti-V5 antibody. Precipitated proteins and whole-cell lysates were probed with antibodies against V5, Myc, Flag, and β-actin. (B) US11 prevents the assembly of TBK1 into the TRIM23-Hsp90 complex. 293T cells were transfected with constructs described above together with or without Flag-US11-mCherry. At 36 h after transfection, cells were processed for immunoprecipitation with anti-V5 antibody. Immunoprecipitates and whole-cell lysates were probed with antibodies against V5, Myc, Flag, and β-actin.

autophagosome formation in TRIM23$^{+/+}$ but not TRIM23$^{-/-}$ cells. Ectopic expression of US11 drastically reduced autophagosome formation. These phenotypes were also recapitulated in TBK1$^{+/+}$ and TBK1$^{-/-}$ cells. Furthermore, when expressed in host cells, US11 associated with TRIM23 in the absence of other viral proteins. Importantly, US11 rescued the viral growth defect imposed by TRIM23. As US11 functionally substituted for $\gamma_1$34.5, these results suggest that at least two separate HSV-1 proteins are required to cope with autophagy-mediated virus restriction. Interpreted within this context, it is noteworthy that in cells infected with wild-type virus $\gamma_1$34.5, expression precedes that of US11. We are inclined to the model that the two proteins act successively as viral infection progresses, which may provide a growth advantage in virus infection.

TRIM23 is a unique E3 ubiquitin ligase that harbors GTPase activity encoded by the C-terminal ARF domain (35, 36). Upon activation, TRIM23 undergoes K27-linked auto-ubiquitination at the ARF domain, which activates the GTPase and subsequently TBK1 enzymatic activity to phosphorylate p62, ultimately promoting autophagy (10). We observed that US11 sharply reduced the number of autophagosomes induced by viral infection or rapamycin stimulation. We further found that US11 was able bind to the

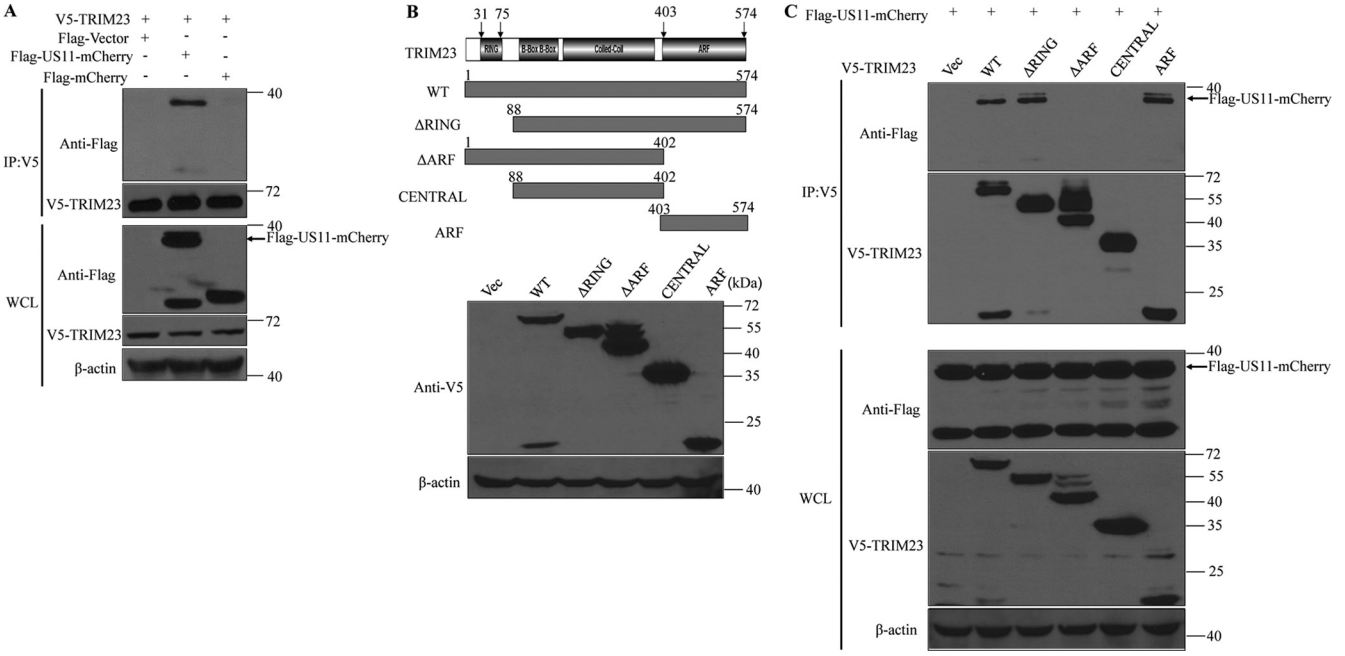

FIG 6 Binding of US11 to TRIM23 requires the ARF domain. (A) The interaction of TRIM23 and US11. 293T cells were transfected with V5-TRIM23 along with Flag-US11-mCherry, Flag-mCherry, or vector plasmid. Cell lysates were processed for immunoprecipitation with anti-V5 and Western blot analysis with antibodies against V5 and Flag. (B) TRIM23 domain structure and mutant constructs. Numbers denote amino acid positions in TRIM23. To verify the expression of TRIM23 variants, 293T cells were transiently transfected with V5-tagged WT TRIM23, ΔRING, ΔARF, CENTRAL, and ARF for 36 h and analyzed by immunoblotting with anti-V5. (C) Binding of US11 to TRIM23 variants. 293T cells were transfected with Flag-US11-mCherry along with V5-TRIM23 WT or its mutants or vector plasmid. At 36 h after transfection, cells were processed for immunoprecipitation with anti-V5 and Western blot analysis with antibodies against V5, Flag, and β-actin.

ARF domain of TRIM23 when expressed in host cells. Although the precise mechanism remains to be fully established, US11 may compete with TBK1 for TRIM23 binding because TRIM23 recruits TBK1 through its ARF domain (10). In line with this model, expression of US11 led to displacement of TBK1 from the TRIM23 complex with little effect on Hsp90. It is further possible that US11 binding to TRIM23 blocks one or multiple ubiquitination sites in the ARF domain, which prevents efficient GTP/GDP cycling of TRIM23 and thereby TBK1 activation. Nevertheless, these working models are not mutually exclusive, and future studies will be needed to define the precise molecular mechanism(s) of US11-mediated inhibition of TRIM23 in the autophagy pathway. Moreover, while our data clearly showed that TBK1 is required for HSV-1-induced autophagy, it is notable that TBK1-independent autophagy exists (37). While intriguing, its relation to TRIM23 is currently unknown and requires further study.

Our work suggests that US11, in addition to disrupting TRIM23-TBK1 complex formation, modulates TRIM23 through an additional mechanism. During virus infection Us11 expression downregulated the steady-state levels of TRIM23. This was evident for both wild-type virus and the US11-expressing virus. Intriguingly, when expressed alone, US11 barely had an effect on TRIM23 protein abundance. US11 similarly modulated TBK1 protein levels but not those of Hsp90. A plausible explanation is that US11 cooperates with another HSV-1 protein(s) to fulfill this task. Alternatively, a separate HSV protein(s) may work independently. The molecular mechanism of how HSV-1 infection leads to reduced TRIM23 protein abundance remains to be determined. Similar to the proteasome-dependent degradation of TBK1 (30), TRIM23 has been suggested to be degraded by the proteasome (38); however, this requires further investigation. On the other hand, many proteins involved in autophagy, such as p62, are degraded by the autophagosome-lysosome degradation pathway. Thus, additional work is necessary to define the degradative pathway(s) utilized by HSV-1 to induce TRIM23 degradation and also to identify the HSV-1 protein responsible for TRIM23 destabilization.

HSV-1 US11 is best characterized for its capacity to inhibit the double-stranded

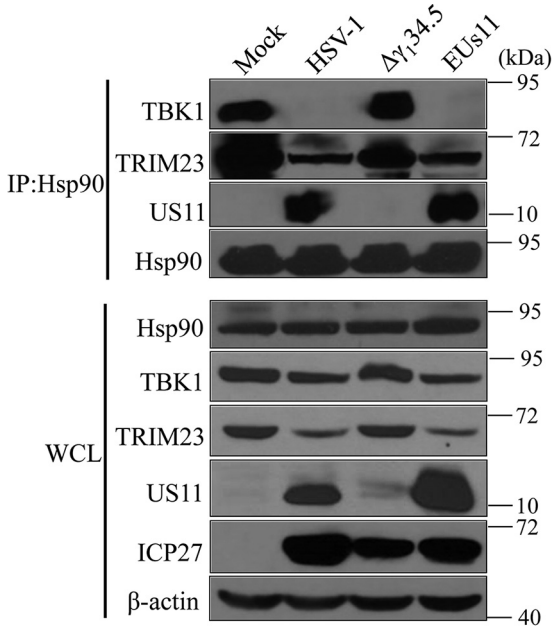

FIG 7 HSV-1 US11 precludes TRIM23-Hsp90-TBK1 ternary complex from forming in infected cells. MEFs were subjected to mock infection or were infected with the indicated viruses (5 PFU/cell). At 12 h postinfection, cells were processed for immunoprecipitation with anti-Hsp90 antibody. Precipitated proteins and whole-cell lysates were probed with antibodies against TRIM23, TBK1, Hsp90, US11, ICP27, and β-actin.

RNA-dependent protein kinase PKR (25–29, 31, 39). The observation that US11 overcomes growth restriction by TRIM23 suggests a previously unrecognized function for this viral protein. Because TRIM23 limits replication of several viruses, including HSV-1 (10), it is not surprising that US11 has evolved to antagonize TRIM23. Exactly how US11 regulates HSV-1 replication remains to be determined. Recent work demonstrates that TRIM23 activates TBK1 (10), an immune kinase that controls autophagy and the type I IFN response (3, 10). We postulate that viral growth rescued by US11 reflects its negative impact on both pathways. Consistent with this idea, we recently noted that US11 inhibits IFN induction mediated by TBK1, which is coupled to viral replication (30). Published work suggests that TRIM23 also regulates other host factors, including I-κB kinase and the adipogenic activator PPARγ (40–42). At this stage, our data do not exclude the possibility that US11 works via an additional pathway(s). Future work will focus on the precise mechanism(s) by which Us11 facilitates viral replication.

MATERIALS AND METHODS

Cells and viruses. Vero, human lung fibroblasts (HEL), and 293T cells were obtained from the American Type Culture Collection. TBK1$^{+/+}$ and TBK1$^{-/-}$ mouse embryonic fibroblasts (MEFs) have been described previously (43). TRIM23$^{+/+}$ and TRIM23$^{-/-}$ MEFs were generous gifts from Martha Vaughn (38). HEL cells stably expressing control short hairpin RNA (shCtrl) or TRIM23-specific short hairpin RNA (shTRIM23) were produced through lentiviral transduction and selection with puromycin (Santa Cruz). MEF cells stably expressing Flag-mCherry and Flag-US11-mCherry were established by lentiviral transduction and selection with puromycin (Santa Cruz). All cells were propagated in Dulbecco's modified Eagle's medium (DMEM) supplemented with 10% fetal bovine serum. HSV-1(F) is a prototype HSV-1 strain used in this study (44). $\Delta\gamma_1$34.5 has deletion of the coding region for the $\gamma_1$34.5 gene (45). EUs11 retains the Us11 gene driven by the α-47 promoter but with the $\gamma_1$34.5 gene removed (30). Preparation of viral stock and titration of infectivity were carried out in Vero cells (43).

Plasmids and reagents. Construction of plasmids Flag-TBK1, Myc-Hsp90, and Myc-EGFP has been described elsewhere (30). Plasmid TRIM23-V5 contains full-length TRIM23 cloned into the XhoI and XbaI sites of pEF-IRES-puro vector (10). The mutants of TRIM23 were generated by PCR and cloned into the XhoI and XbaI sites in pEF-IRES-puro vector (38). Specifically, ΔRING expresses amino acids 88 to 574 of TRIM23, ΔARF expresses amino acids 1 to 402, CENTRAL encodes amino acids 88 to 402, and ARF expresses amino acids 403 to 574. Plasmid GFP-LC3B was obtained from Yoshinori Ohsumi. Plasmid Flag-mCherry was constructed by inserting a PCR-amplified fragment into the EcoRV and XhoI sites of pCDH-Flag. For Flag-US11-mCherry, a PCR fragment of the Us11 gene was cloned into the BamHI and

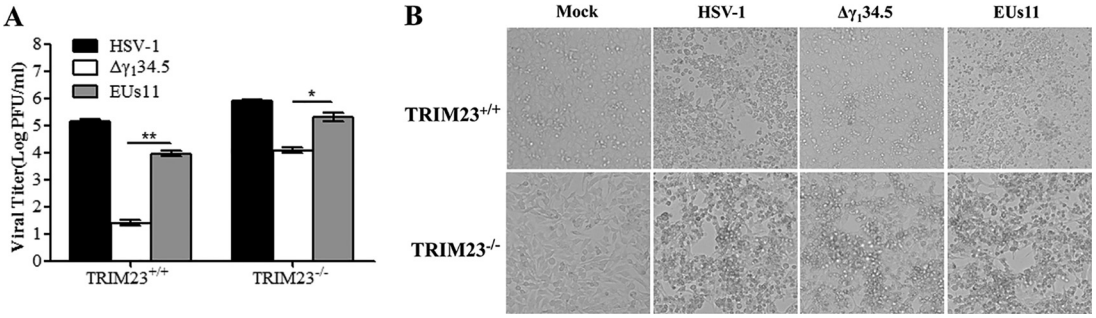

FIG 8 (A) Viral replication in TRIM23$^{+/+}$ or TRIM23$^{-/-}$ cells. Cells were infected with wild-type HSV-1, $\Delta\gamma_1$34.5, or EUs11 at 0.01 PFU per cell. At 48 h postinfection, cells were harvested and the total virus yields were determined by plaque assay on Vero cells. (B) Virus-induced cytopathic effects in TRIM23$^{+/+}$ and TRIM23$^{-/-}$ cells. Cytopathic effects in cells infected as described for panel A were visualized by microcopy. The data are representative of three independent experiments from triplicate samples and assessed by a two-tailed Student's *t* test (**, $P < 0.01$; *, $P < 0.5$).

EcoRV sites in Flag-mCherry. pLKO.1-puro vector-based shRNA expression cassettes for TRIM23 (sense sequence, CCGGGCTTGG AAGAAGGTTG TCAAACTCGA GTTTGACAAC CTTCTTCCAA GCTTTTTG) and the control (sense sequence, CCTAAGGTTA AGTCGCCCTC GCTCGAGCGA GGGCGACTTA ACCTTAGG) were purchased from Sigma. Rapamycin was purchased from Santa Cruz (number 53123-88-9) and used as a positive control to induce the autophagy at a concentration of 200 nM.

Viral infection assay. Cells were mock infected or infected with viruses. At the indicated time point, cells were harvested and processed for Western blot and immunoprecipitation analyses. For cytoplasmic GFP-LC3B puncta visualization, GFP-LC3B was transfected into the cells. After 24 h, the cells were mock infected or infected with viruses. At 12 h postinfection, the cells were fixed for confocal microscopy analysis. To assay for viral growth, infected cells were harvested and freeze-thawed three times. Viral yields were determined on Vero cells at 37°C (43).

Immunoprecipitation analysis. 293T cells were transfected with Lipofectamine 3000 (Invitrogen) according to the manufacturer's instruction for 36 h. Alternatively, MEF cells were mock infected or infected with viruses for 12 h. Immunoprecipitation was carried out as described previously (46). Briefly, cells were harvested and lysed with ice-cold immunoprecipitation buffer. After centrifugation, cell extracts were incubated with the indicated antibodies and agarose conjugated with protein A/G at 4°C. The immobilized protein beads were subjected to electrophoresis and immunoblot analysis.

Immunoblot analysis. MEF and HEL cells were mock infected or infected with viruses. At 12 h postinfection, cells were harvested and lysed with ice-cold 50 mM Tris-Cl buffer (30). Samples were then separated by electrophoresis, transferred to nitrocellulose membranes, and reacted with antibodies against TBK1 (number 3504; Cell Signaling Technology), TRIM23 (ab192032; Abcam), TRIM23 (sc-135587; Santa Cruz), LC3B (number 3868; Cell Signaling Technology), Hsp90 (sc-13119; Santa Cruz), β-actin (Sigma), US11 (47), ICP27 (Virusys, Inc.), anti-V5 (sc-271944; Santa Cruz), anti-Myc (sc-40; Santa Cruz), anti-Flag-horseradish peroxidase (anti-Flag-HRP) (Sigma), or anti-Myc-HRP (Cell Signaling Technology). The membranes were rinsed in phosphate-buffered saline and reacted with either donkey anti-rabbit (Santa Cruz) or donkey anti-mouse (Santa Cruz) immunoglobulin conjugated to HRP and developed with an enhanced chemiluminescence Western blot detection system kit (Amersham Pharmacia Biotechnology).

Confocal microscopy. MEF cells were grown on coverslips (Chemglass) and transfected with plasmid GFP-LC3B using Lipofectamine 3000 (Invitrogen) according to the manufacturer's instructions. Cells were fixed with 4% (wt/vol) paraformaldehyde (Santa Cruz) for 20 min. Cells were mounted in 4′,6-diamidino-2-phenylindole (DAPI)-containing Vectashield (Vector Labs) to costain nuclei. All laser scanning images were acquired on a Zeiss LSM710 confocal microscope and processed with Zen 2010 software (Zeiss). Cytoplasmic GFP-LC3B puncta in cells were manually counted for at least 20 randomly selected cells.

ACKNOWLEDGMENTS

This work was supported in part by grants from the National Institute of Allergy and Infectious Diseases (AI119618 to B.H. and AI087846 to M.U.G.).

We thank Bernard Roizman, Martha Vaughn, and Yoshinori Ohsumi for providing valuable reagents.

REFERENCES

1. Virgin HW, Levine B. 2009. Autophagy genes in immunity. Nat Immunol 10:461–470. https://doi.org/10.1038/ni.1726.
2. Levine B, Kroemer G. 2019. Biological functions of autophagy genes: a disease perspective. Cell 176:11–42. https://doi.org/10.1016/j.cell.2018.09.048.
3. Ahmad L, Zhang SY, Casanova JL, Sancho-Shimizu V. 2016. Human TBK1: a gatekeeper of neuroinflammation. Trends Mol Med 22:511–527. https://doi.org/10.1016/j.molmed.2016.04.006.
4. Chou J, Chen JJ, Gross M, Roizman B. 1995. Association of a M(r) 90,000 phosphoprotein with protein kinase PKR in cells exhibiting enhanced

phosphorylation of translation initiation factor eIF-2 alpha and premature shutoff of protein synthesis after infection with $g_1$34.5- mutants of herpes simplex virus 1. Proc Natl Acad Sci U S A 92:10516–10520. https://doi.org/10.1073/pnas.92.23.10516.
5. Chou J, Roizman B. 1992. The γ134.5 gene of herpes simplex virus 1 precludes neuroblastoma cells from triggering total shutoff of protein synthesis characteristic of programed cell death in neuronal cells. Proc Natl Acad Sci U S A 89:3266–3270. https://doi.org/10.1073/pnas.89.8.3266.
6. Talloczy Z, Jiang W, Virgin HWT, Leib DA, Scheuner D, Kaufman RJ, Eskelinen EL, Levine B. 2002. Regulation of starvation- and virus-induced autophagy by the eIF2alpha kinase signaling pathway. Proc Natl Acad Sci U S A 99:190–195. https://doi.org/10.1073/pnas.012485299.
7. Shen S, Niso-Santano M, Adjemian S, Takehara T, Malik SA, Minoux H, Souquere S, Marino G, Lachkar S, Senovilla L, Galluzzi L, Kepp O, Pierron G, Maiuri MC, Hikita H, Kroemer R, Kroemer G. 2012. Cytoplasmic STAT3 represses autophagy by inhibiting PKR activity. Mol Cell 48:667–680. https://doi.org/10.1016/j.molcel.2012.09.013.
8. Sharma S, tenOever BR, Grandvaux N, Zhou GP, Lin R, Hiscott J. 2003. Triggering the interferon antiviral response through an IKK-related pathway. Science 300:1148–1151. https://doi.org/10.1126/science.1081315.
9. McWhirter SM, Fitzgerald KA, Rosains J, Rowe DC, Golenbock DT, Maniatis T. 2004. IFN-regulatory factor 3-dependent gene expression is defective in Tbk1-deficient mouse embryonic fibroblasts. Proc Natl Acad Sci U S A 101:233–238. https://doi.org/10.1073/pnas.2237236100.
10. Sparrer KMJ, Gableske S, Zurenski MA, Parker ZM, Full F, Baumgart GJ, Kato J, Pacheco-Rodriguez G, Liang C, Pornillos O, Moss J, Vaughan M, Gack MU. 2017. TRIM23 mediates virus-induced autophagy via activation of TBK1. Nat Microbiol 2:1543–1557. https://doi.org/10.1038/s41564-017-0017-2.
11. Cunningham AL, Diefenbach RJ, Miranda-Saksena M, Bosnjak L, Kim M, Jones C, Douglas MW. 2006. The cycle of human herpes simplex virus infection: virus transport and immune control. J Infect Dis 194(Suppl 1):S11–18. https://doi.org/10.1086/505359.
12. Whitley RJ, Roizman B. 2001. Herpes simplex virus infections. Lancet 357:1513–1518. https://doi.org/10.1016/S0140-6736(00)04638-9.
13. He B, Gross M, Roizman B. 1997. The $g_1$34.5 protein of herpes simplex virus 1 complexes with protein phosphatase 1alpha to dephosphorylate the alpha subunit of the eukaryotic translation initiation factor 2 and preclude the shutoff of protein synthesis by double-stranded RNA-activated protein kinase. Proc Natl Acad Sci U S A 94:843–848. https://doi.org/10.1073/pnas.94.3.843.
14. He B, Gross M, Roizman B. 1998. The γ134.5 protein of herpes simplex virus 1 has the structural and functional attributes of a protein phosphatase 1 regulatory subunit and is present in a high molecular weight complex with the enzyme in infected cells. J Biol Chem 273:20737–20743. https://doi.org/10.1074/jbc.273.33.20737.
15. Orvedahl A, Alexander D, Talloczy Z, Sun Q, Wei Y, Zhang W, Burns D, Leib DA, Levine B. 2007. HSV-1 ICP34.5 confers neurovirulence by targeting the Beclin 1 autophagy protein. Cell Host Microbe 1:23–35. https://doi.org/10.1016/j.chom.2006.12.001.
16. Leib DA, Alexander DE, Cox D, Yin J, Ferguson TA. 2009. Interaction of ICP34.5 with Beclin 1 modulates herpes simplex virus type 1 pathogenesis through control of CD4+ T-cell responses. J Virol 83:12164–12171. https://doi.org/10.1128/JVI.01676-09.
17. Gobeil PA, Leib DA. 2012. Herpes simplex virus gamma34.5 interferes with autophagosome maturation and antigen presentation in dendritic cells. mBio 3:e00267. https://doi.org/10.1128/mBio.00267-12.
18. Lussignol M, Queval C, Bernet-Camard MF, Cotte-Laffitte J, Beau I, Codogno P, Esclatine A. 2013. The herpes simplex virus 1 Us11 protein inhibits autophagy through its interaction with the protein kinase PKR. J Virol 87:859–871. https://doi.org/10.1128/JVI.01158-12.
19. Johnson PA, MacLean C, Marsden HS, Dalziel RG, Everett RD. 1986. The product of gene US11 of herpes simplex virus type 1 is expressed as a true late gene. J Gen Virol 67:871–883. https://doi.org/10.1099/0022-1317-67-5-871.
20. Roller RJ, Roizman B. 1990. The herpes simplex virus Us11 open reading frame encodes a sequence-specific RNA-binding protein. J Virol 64:3463–3470.
21. Sanchez R, Mohr I. 2007. Inhibition of cellular 2′-5′ oligoadenylate synthetase by the herpes simplex virus type 1 Us11 protein. J Virol 81:3455–3464. https://doi.org/10.1128/JVI.02520-06.
22. Kew C, Lui PY, Chan CP, Liu X, Au SW, Mohr I, Jin DY, Kok KH. 2013. Suppression of PACT-induced type I interferon production by herpes simplex virus 1 Us11 protein. J Virol 87:13141–13149. https://doi.org/10.1128/JVI.02564-13.
23. Xing J, Wang S, Lin R, Mossman KL, Zheng C. 2012. Herpes simplex virus 1 tegument protein US11 downmodulates the RLR signaling pathway via direct interaction with RIG-I and MDA-5. J Virol 86:3528–3540. https://doi.org/10.1128/JVI.06713-11.
24. Javouhey E, Gibert B, Arrigo AP, Diaz JJ, Diaz-Latoud C. 2008. Protection against heat and staurosporine mediated apoptosis by the HSV-1 US11 protein. Virology 376:31–41. https://doi.org/10.1016/j.virol.2008.02.031.
25. Poppers J, Mulvey M, Khoo D, Mohr I. 2000. Inhibition of PKR activation by the proline-rich RNA binding domain of the herpes simplex virus type 1 Us11 protein. J Virol 74:11215–11221. https://doi.org/10.1128/JVI.74.23.11215-11221.2000.
26. Peters GA, Khoo D, Mohr I, Sen GC. 2002. Inhibition of PACT-mediated activation of PKR by the herpes simplex virus type 1 Us11 protein. J Virol 76:11054–11064. https://doi.org/10.1128/jvi.76.21.11054-11064.2002.
27. Mohr I, Gluzman Y. 1996. A herpesvirus genetic element which affects translation in the absence of the viral GADD34 function. EMBO J 15:4759–4766. https://doi.org/10.1002/j.1460-2075.1996.tb00853.x.
28. Cassady KA, Gross M, Roizman B. 1998. The herpes simplex virus US11 protein effectively compensates for the g134.5 gene if present before activation of protein kinase R by precluding its phosphorylation and that of the alpha subunit of eukaryotic translation initiation factor 2. J Virol 72:8620–8626.
29. Cassady KA, Gross M, Roizman B. 1998. The second-site mutation in the herpes simplex virus recombinants lacking the g134.5 genes precludes shutoff of protein synthesis by blocking the phosphorylation of eIF-2alpha. J Virol 72:7005–7011.
30. Liu X, Main D, Ma Y, He B. 2018. Herpes simplex virus 1 inhibits TANK-binding kinase 1 through formation of the Us11-Hsp90 complex. J Virol 92:e00402-18. https://doi.org/10.1128/JVI.00402-18.
31. Mulvey M, Camarena V, Mohr I. 2004. Full resistance of herpes simplex virus type 1-infected primary human cells to alpha interferon requires both the Us11 and gamma(1)34.5 gene products. J Virol 78:10193–10196. https://doi.org/10.1128/JVI.78.18.10193-10196.2004.
32. Mulvey M, Poppers J, Sternberg D, Mohr I. 2003. Regulation of eIF2alpha phosphorylation by different functions that act during discrete phases in the herpes simplex virus type 1 life cycle. J Virol 77:10917–10928. https://doi.org/10.1128/jvi.77.20.10917-10928.2003.
33. Lee MN, Roy M, Ong SE, Mertins P, Villani AC, Li W, Dotiwala F, Sen J, Doench JG, Orzalli MH, Kramnik I, Knipe DM, Lieberman J, Carr SA, Hacohen N. 2013. Identification of regulators of the innate immune response to cytosolic DNA and retroviral infection by an integrative approach. Nat Immunol 14:179–185. https://doi.org/10.1038/ni.2509.
34. Yang K, Shi H, Qi R, Sun S, Tang Y, Zhang B, Wang C. 2006. Hsp90 regulates activation of interferon regulatory factor 3 and TBK-1 stabilization in Sendai virus-infected cells. Mol Biol Cell 17:1461–1471. https://doi.org/10.1091/mbc.e05-09-0853.
35. Vitale N, Moss J, Vaughan M. 1996. ARD1, a 64-kDa bifunctional protein containing an 18-kDa GTP-binding ADP-ribosylation factor domain and a 46-kDa GTPase-activating domain. Proc Natl Acad Sci U S A 93:1941–1944. https://doi.org/10.1073/pnas.93.5.1941.
36. Vichi A, Moss J, Vaughan M. 2005. ADP-ribosylation factor domain protein 1 (ARD1), a multifunctional protein with ubiquitin E3 ligase, GAP, and ARF domains. Methods Enzymol 404:195–206. https://doi.org/10.1016/S0076-6879(05)04019-X.
37. Gui X, Yang H, Li T, Tan X, Shi P, Li M, Du F, Chen ZJ. 2019. Autophagy induction via STING trafficking is a primordial function of the cGAS pathway. Nature 567:262–266. https://doi.org/10.1038/s41586-019-1006-9.
38. Meza-Carmen V, Pacheco-Rodriguez G, Kang GS, Kato J, Donati C, Zhang CY, Vichi A, Payne DM, El-Chemaly S, Stylianou M, Moss J, Vaughan M. 2011. Regulation of growth factor receptor degradation by ADP-ribosylation factor domain protein (ARD) 1. Proc Natl Acad Sci U S A 108:10454–10459. https://doi.org/10.1073/pnas.1103867108.
39. He B, Chou J, Brandimarti R, Mohr I, Gluzman Y, Roizman B. 1997. Suppression of the phenotype of g134.5- herpes simplex virus 1: failure of activated RNA-dependent protein kinase to shut off protein synthesis is associated with a deletion in the domain of the alpha47 gene. J Virol 71:6049–6054.
40. Arimoto K, Funami K, Saeki Y, Tanaka K, Okawa K, Takeuchi O, Akira S, Murakami Y, Shimotohno K. 2010. Polyubiquitin conjugation to NEMO by triparite motif protein 23 (TRIM23) is critical in antiviral defense. Proc Natl Acad Sci U S A 107:15856–15861. https://doi.org/10.1073/pnas.1004621107.

41. Laurent-Rolle M, Morrison J, Rajsbaum R, Macleod JML, Pisanelli G, Pham A, Ayllon J, Miorin L, Martinez C, tenOever BR, García-Sastre A. 2014. The interferon signaling antagonist function of yellow fever virus NS5 protein is activated by type I interferon. Cell Host Microbe 16:314–327. https://doi.org/10.1016/j.chom.2014.07.015.
42. Watanabe M, Takahashi H, Saeki Y, Ozaki T, Itoh S, Suzuki M, Mizushima W, Tanaka K, Hatakeyama S. 2015. The E3 ubiquitin ligase TRIM23 regulates adipocyte differentiation via stabilization of the adipogenic activator PPARgamma. Elife 4:e05615. https://doi.org/10.7554/eLife.05615.
43. Verpooten D, Ma Y, Hou S, Yan Z, He B. 2009. Control of TANK-binding kinase 1-mediated signaling by the $g_1$34.5 protein of herpes simplex virus 1. J Biol Chem 284:1097–1105. https://doi.org/10.1074/jbc.M805905200.
44. Ejercito PM, Kieff ED, Roizman B. 1968. Characterization of herpes simplex virus strains differing in their effects on social behaviour of infected cells. J Gen Virol 2:357–364. https://doi.org/10.1099/0022-1317-2-3-357.
45. Chou J, Kern ER, Whitley RJ, Roizman B. 1990. Mapping of herpes simplex virus-1 neurovirulence to gamma 134.5, a gene nonessential for growth in culture. Science 250:1262–1266. https://doi.org/10.1126/science.2173860.
46. Ma Y, Jin H, Valyi-Nagy T, Cao Y, Yan Z, He B. 2012. Inhibition of TANK binding kinase 1 by herpes simplex virus 1 facilitates productive infection. J Virol 86:2188–2196. https://doi.org/10.1128/JVI.05376-11.
47. Roller RJ, Roizman B. 1992. The herpes simplex virus 1 RNA binding protein US11 is a virion component and associates with ribosomal 60S subunits. J Virol 66:3624–3632.